AMIP NEWSLETTER

No. 6 WGNE Atmospheric Model Intercomparison Project February 1995

An information summary and activities description for the Atmospheric Model Intercomparison Project (AMIP) of the Working Group on Numerical Experimentation (WGNE) in support of the World Climate Research Programme. Technical and computational support for AMIP is being provided by the Environmental Sciences Division of the U.S. Department of Energy through the Program for Climate Model Diagnosis and Intercomparison (PCMDI) at the Lawrence Livermore National Laboratory (LLNL), where this Newsletter is edited by Larry Gates, Chairman, WGNE AMIP Panel, PCMDI, L-264, LLNL, P.O. Box 808, Livermore, CA 94550, USA.

AMIP Update

A significant AMIP milestone has now been reached with the completion of the 1979-88 simulation by all of the currently participating modeling groups. As shown in the table on page 5, the monthly-averaged AMIP Standard Output for the 30 participating models has now been quality-controlled and is available for distribution. The AMIP daily history has been quality-controlled for only three models, although the history for 4 additional models is expected to be ready in the near future. These data are available to the AMIP Diagnostic Subprojects by mail or electronic transfer from the AMIP archives maintained at Livermore by PCMDI (see page 20 for contacts). The table on page 5 also serves to identify the specific model version that has been used in each modeling group's initial AMIP simulation, and corresponds to the AMIP model documentation that has recently been completed by Tom Phillips (PCMDI Report No. 18, 1994, 343 pp.); copies of this report are available upon request, and are expected to be available electronically in 1995.

AMIP Ensembles and Revisits

Although mentioned in AMIP Newsletter No. 5 (January 1994), all participating modeling groups are requested to submit the Standard Output from additional runs for the 1979–88 decade made with alternative initial conditions with their original AMIP models. The results of such AMIP model ensembles are useful for the study of natural variability and potential predictability, and are a valuable addition to the AMIP data archives.

It is also requested that the monthly-averaged Standard Output from integrations over the AMIP decade made with revised versions of the original AMIP models be submitted to PCMDI, along with a documentation of the model revisions. These results will be useful in the validation of specific model improvements, will permit a summary of the performance of "second generation" AMIP models, and will enable the AMIP Diagnostic Subprojects to update their analyses. The history from such runs is also welcome, although a backlog of such data from the original models is already on hand (see table on page 5). It is anticipated that PCMDI's ability to handle such data will be significantly increased with the acquisition of greatly expanded storage in 1995.

AMIP Validation Data

A review of PCMDI's observational data for the validation of AMIP model performance (as described in AMIP Newsletter No. 5, January 1994) has revealed that many of the "traditional" data sets were outdated and/or inconsistent in structure and quality. New and improved versions of these and other global datasets have now been acquired, as summarized in the table on page 2.

AMIP Validation Data

Data Set	*Period*	*Source*
Upper air analyses	1979–1989	GFDL/Oort
Diagnostic analyses	1979–present	NOAA/CAC
ECMWF TOGA analyses	1985–1991	NASA/DAO
Hydrology (sfc. temp., precip., soil moisture)	1978–1992	NASA/DAO
MSU precipitation	1979–present	NASA/MSFC
COADS/Univ. Wisc. Milw. (ocean sfc. flux)	Climatology	NASA/DAO
SSM/I hydrology (precip., cl. liq. water, snow, sea ice)	1987–present	NOAA/NESDIS
NMC/NCAR reanalysis	1985–1991	NOAA/NMC
NRL reanalysis	1985–1989	NRL/Monterey
NASA reanalysis	1985–1992	NASA/DAO

All of these data sets contain monthly means over the indicated period, with the GFDL, NOAA, and NASA analyses also containing the variance and the MSU data also containing the daily mean precipitation. The three reanalysis data sets also contain daily and/or 6-hourly values, and will be extended to 1979 whenever possible; data from the ECMWF reanalysis will also be acquired in 1995.

Consistent with PCMDI's objective to provide the AMIP community with observational data in a consistent and easily accessible form with which to validate and diagnose models over the AMIP period, routines are being developed to permit regridding to specific model grids, and to permit access in a variety of formats with simple code and/or interfaces to other processing/display systems. It is planned to produce an initial release of AMIP observational data in the form of a CD-ROM by the time of the AMIP Scientific Conference in May 1995 (see page 3). In the meantime, AMIP participants may request information and selected data sets from Mike Fiorino at fiorino@typhoon.llnl.gov

PCMDI Software

Part of PCMDI's mission is the development of software for the storage and display of climate model results. While the earlier DRS and MAP software are being used by several AMIP participants, here we report to the AMIP community at large the progress that has been made in extending these packages and their availability.

DRS—The Data Retrieval and Storage Library

The DRS library is a software library that defines a data format and access methods that are tailored for the data used in climate model diagnosis and intercomparison. DRS is well suited for research that requires the storage of very large multi-dimensional datasets on supercomputers, as well as in studies that access subsets of such data for analysis and display. The basic DRS library (described in PCMDI Report No. 16, March 1994) has been upgraded to run on Sun/Sun OS, Sun/Solaris, CRAY/Unicos, SGI/Irix and HP9000/HP-UX systems, and is available to AMIP participants and PCMDI collaboration upon request from Bob Drach at drach@cricket.llnl.gov

VCS—The Visualization and Computation System

The VCS software was designed to provide flexible capabilities for visualizing climate data and for performing some of the basic computations involved in climate model diagnosis, validation, and intercomparison. The basic VCS package (described in PCMDI Report No. 17, March 1994) currently runs on Sun/SunOS, Sun/Solaris and SGI/Irix, and allows user control of graphics, text, color and animation, and supports grid manipulation and data computation. VCS can be controlled interactively through a Motif interface or from a script file (or alternatively between these modes during a session), and has the capability to create and control all aspects of a display (including line diagrams, contours, vectors, and color). VCS can also browse and extract stored variables, manipulate their dimensions, create output files, and run and/or create scripts and sequences of graphic images for animation. The VCS software is currently being beta-tested at PCMDI, and will be released to the AMIP community early in 1995; this version is expected to allow the ingestion of several data formats, including NetCDF and GrADS/GRIB, in addition to DRS. Further information on VCS can be obtained from either Bob Mobley at mobley@rabbitt.llnl.gov or Dean Williams at williams@asia.llnl.gov

DDI—The Data and Dimensions Interface

A long-standing problem in the visualization of large climate (and other) datasets is the extraction of only the relevant data and delivering them in the desired form in an efficient manner. The newly-developed DDI addresses this need by providing an interactive Motif interface that transfers data between files, formats and local or remote visualization systems. DDI has the capability to browse data files, randomly select variables, to manipulate the data dimensions, and to rearrange them in new files for input into visualization systems. Although undergoing further development, DDI can currently service a variety of visualization systems, including PCMDI's VCS, the Application Visualization System (AVS) from Advanced Visual Systems, Inc., IRIS Explorer from the Numerical Algorithms Group (NAG) Ltd., PV-WAVE from Visual Numerics, Inc., the Interactive Data Language (IDL) from Research Systems, Inc., and Collage and XImage from NCSA. The current version of DDI is available via anonymous FTP from "sas.nersc.gov" in the directory "/pub/DDI". The "Introduction to DDI" and the "DDI Reference Manual" are available via HTML: "http://www.nersc.gov/doc/Services/Applications/Graphics/DDI/DDI.html" and can be viewed with MOSAIC.

CDMS—The Climate Data Management System

The archive of climate model and observational datasets at PCMDI now comprises over three terabytes of data. To make these data as easy to use and manage as possible, the CDMS is being developed to provide a uniform view of the data as logical collections independent of underlying physical representation and location. Notable features of CDMS include support for four-dimensional data arrays in either spectral or gridded representations, access to data by uniform C and FORTRAN application programming interfaces (as well as by an enhanced version of the DDI browser described above), data storage either internal to the database or in external files in any of several formats including DRS, GrADS (GRIB or binary) and NetCDF, and datasets with standardized variable names and units residing on multiple devices and file systems. CDMS is compatible with the NEONS data management system developed at the Naval Research Laboratory in Monterey, California. Further information on the CDMS can be obtained from Bob Drach at drach@cricket.llnl.gov

The PCMDI-developed software described above will be made available to the AMIP community in 1995. It is also anticipated that portions of the PCMDI library of statistical and diagnostic software now under development will be accessible as they are completed and tested. Information on these software packages can be obtained from Ben Santer (statistics) at bsanter@rainbow.llnl.gov or from Jim Boyle (diagnostics) at boyle@cobra.llnl.gov

AMIP Scientific Conference

An AMIP Scientific Conference under the sponsorship of the World Climate Research Programme and the Program for Climate Model Diagnosis and Intercomparison of the U.S. Department of Energy, will be held 15–19 May 1995 at the U.S. Naval Postgraduate School in Monterey, California. Based on the response to the preliminary solicitation of interest that was widely distributed in October 1994, an attendance of approximately 150 is expected, including representatives from each of the modeling groups and diagnostic subprojects participating in AMIP as well as representatives from other climate model diagnostic and intercomparison activities. It is planned to publish the conference proceedings in the WCRP report series, for which speakers will be asked to submit their reports either before or as soon after the conference as possible. Although analysis and diagnosis of the AMIP simulations made with both the original and revised atmospheric models will continue, this (first) AMIP Scientific Conference is expected to produce a valuable summary of the AMIP experience to date. Further information on the conference will be distributed in the near future by the Conference Organizing Committee.

AMIP Contribution to IPCC

Many participants in AMIP are contributing as individuals to the Second Scientific Assessment of Climate Change that is currently being assembled by the Intergovernmental Panel on Climate Change (IPCC). In order to promote the use of the AMIP simulations in the validation of atmospheric GCMs, Larry Gates has agreed to act as the convening lead author (with back-up by Ann Henderson-Sellers) for a chapter on climate model validation in the 1995 IPCC report. With the help of Mike Fiorino and other PCMDI staff, Larry will use the AMIP database to discuss the mean errors and standard deviation among the AMIP models in simulating the seasonal cycle of selected near-surface variables.

Update of Addresses of AMIP Modeling Group Representatives and Diagnostic Subproject Leaders

Changes and additions to the addresses listed on pp. 10–14 of AMIP Newsletter No. 5 (January 1994) are given below.

CNRM
Dr. Michel Déqué
Centre National de
Recherches Meteorologiques
42 Avenue Coriolis
31057 Toulouse Cedex
France
Tel: 33 61 07 93 77
FAX: 33 61 07 96 10
email: michel.deque@meteo.fr

UKMO
Mr. Christopher D. Hall
Hadley Centre for Climate
Prediction and Research
U.K. Meteorological Office
London Road
Bracknell, Berkshire RG12 2SY
United Kingdom
Tel: 44 344 854490
FAX: 44 344 854898
email: cdhall@email.meto.govt.uk

DS23
Dr. Sultan Hameed
Institute for Terrestrial and Planetary
Atmospheres
Marine Sciences Research Center
State University of New York
at Stony Brook
Stony Brook, NY 11794-5000
Tel: (516) 632-8319
FAX: (516) 632-8379
email: hameed@atmsci.sunysb.edu

DS24
Dr. George S. Golitsyn
Institute for Atmospheric Physics
Russian Academy of Sciences
3 Pyzhevsky
Moscow 109017
Russia
FAX: 7 095 233 1652
email: iaph!root@kremvax.demos.su

DS25
Dr. Wei-Chyung Wang
Atmospheric Sciences
Research Center
State University of New York
at Albany
100 Fuller Road
Albany, NY 12205
Tel: (518) 442-3357
FAX: (518) 442-3360
email: wang@climate.asrc.albany.edu

DS26
Dr. Sulochana Gadgil
Centre for Atmospheric Sciences
Indian Institute of Science
Bangalore 560 012
India
FAX: 080 344 1683
email:sulo@cas.iisc.ernet.in

AMIP Models and Output Status

Group	Contact(s)	Model Version	Resolution	Standard Output	History
BMRC	McAvaney	BMRC 2.3	R31 L9	completed	Δ
CCC	Boer	GCM II	T32 L10	completed	
CNRM	Déqué	EMERAUDE	T42 L30	completed	
COLA	Straus	COLA 1.1	R40 L18	completed	
CSIRO	Hunt	CSIRO 9 Mark 1	R21 L9	completed	completed
CSU	Randall	CSU 91	4x5 L17	completed	completed
DERF	Miyakoda	GFDL SM392.2	T42 L18	completed	Δ
DNM	Galin	A5407.VI	4x5 L7	completed	
ECMWF	Ferranti	ECMWF Cy36	T42 L19	completed	completed
GFDL	Wetherald	CDG 1	R30 L14	completed	
GISS	Lo/Del Genio	MODEL II Prime	4x5 L9	completed	
GLA	Lau	GCM-01.0 AMIP-01	4x5 L17	completed	
GSFC	Park	GEOS-1	4x5 L20	completed	
IAP	Wang/Zeng	IAP-2L	4x5 L2	completed	
JMA	Sato	GSM 8911	T42 L21	completed	
LMD	Le Treut	LMD 5	3.6x5.6 L11	completed	
MGO	Meleshko	AMIP 92	T30 L14	completed	
MPI	Dümenil/Schlese	ECHAM 3	T42 L19	completed	
MRI	Kitoh	GCM-II	4x5 L15	completed	Δ
NCAR	Williamson	CCM2	T42 L18	completed	
NMC	van den Dool	MRF	T40 L18	completed	
NRL	Rosmond	NOGAPS 3.2	T47 L18	completed	
RPN	Ritchie	NWP-D40P29	T63 L23	completed	
SUNYA	Wang	CCM1-TG	R15 L12	completed	
SUNYA/NCAR	Wang/Thompson	GENESIS 1.5	T31 L18	completed	
UCLA	Mechoso	AGCM 6.4	4x5 L15	completed	
UGAMP	Blackburn/Slingo	UGCM 1.3	T42 L19	completed	
UIUC	Schlesinger	MLAM-AMIP	4x5 L7	completed	
UKMO	Hall	UM-CLIMATE1	2.5x3.75 L19	completed	Δ
YONU	Oh	Tr 5.1	4x5 L5	completed	

Δ denotes standard output/history undergoing quality control at PCMDI

AMIP Diagnostic Subprojects

A total of twenty-six diagnostic subprojects have now been established (see table below). Instead of distributing only the standard output specifically requested by each subproject as originally envisaged, the complete set of standard output for all models is now available to the subprojects (as well as to the modeling groups themselves) upon request. It is assumed, however, that each subproject will maintain its approved focus and will not undertake analyses that are the primary responsibility of another subproject without appropriate coordination. The subprojects are also reminded of their responsibility to prepare in due course a report for the WCRP report series and to submit their results to PCMDI for archival storage.

An update of the AMIP modeling groups' participation in the diagnostic subprojects is given in the table on page 7. Many modeling groups have designated specific persons to serve as their contacts with those subprojects in which they are actively participating, and this list is available upon request. While proposals for additional diagnostic subprojects are welcome from either the modeling or diagnostics community, the AMIP Panel urges that further diagnoses and validation be carried out in cooperation with the existing subprojects whenever feasible. Brief descriptions of the preliminary results from selected subprojects are given on pp. 8–19.

Number	Leader(s)	Short Title	Data Needs	
			Std. Output	History
1	J. Slingo (UGAMP)	Synoptic variability	–	6 hr
2	Zwiers (CCC)	Low frequency variability	–	24 hr
3	Lambert (CCC)	Cyclone frequency	–	12 hr
4	Duvel (LMD)/Cheruy (LMD)	Greenhouse sensitivity	x	6 hr
5	Randall (CSU)	Surface ocean fluxes	x	–
6	Palmer (ECMWF)	Monsoons(1) 1)	x	6 hr
7	Lau (GLA)	Hydrologic processes	x	6 hr
8	Walsh (UIUC)	Polar processes(2)	x	24 hr
9	McAvaney (BMRC)	S.H. circulation	x	6 hr
10	Tibaldi (ADGB)	Blocking	–	24 hr
11	Robock (UMD)	Soil moisture	x	6 hr
12	Henderson-Sellers (MACU)	Land surface processes(3)	x	6 hr
13	Weare (UCD)/Mokhov (RAS)	Cloudiness	x	–
14	Potter (PCMDI)	Cloud forcing	x	6 hr
15	Hide (UKMO/JPL)	Angular momentum	–	6 hr
16	Mechoso (UCLA)	Stratospheric circulation	–	24 hr
17	Robertson (MSFC)	Water, energy balance(4)	x	6 hr
18	Meleshko (MGO)	Extreme events	x	–
19	Christy (UAL)	MSU validation	x	6 hr
20	Hewitson (UCT)	S.H./S. Africa circulation	–	12 hr
21	Jones (CRU)	Surface climatologies	x	24 hr
22	Tanaka (UTSU)	Energetics	–	12 hr
23	Hameed (SUNYSB)	Centers of action	x	24 hr
24	Golitsyn (RAS)	Caspian Sea	x	24 hr
25	Wang (SUNYA)	East Asian climate	x	24 hr
26	Gadgil (IIS)	Monsoon precipitation(5)	x	–

---

(1) coordinated with MONEG/TOGA, GOALS/CLIVAR

(2) coordinated with SIOMP/ACSYS

(3) coordinated with PILPS/GEWEX

(4) coordinated with GCIP/GEWEX

(5) coordinated with START

Modeling Group Participation in Diagnostic Subprojects

AMIP Diagnostic Subproject Number (see table on page 6)

	1	2	3	4	5	6	7	8	9	10	11	12	13	14	15	16	17	18	19	20	21	22	23	24	25	26
BMRC	+	–	–	+	+	+	+	+	+	+	+	+	–	+	+	–	–	–	+	+	–	+	–	–		
CCC	+	+	+	+	+	+	+	+	–	–	–	–	–	–	+	–	–	–	–	–	–	+	–	–	+	+
CNRM	+	+	–	–	+	–	+	–	+	–	+	+	–	–	–	+	–	–	–	–	–	–	–	–	–	+
COLA	–	+	–	–	–	+	–	–	–	+	–	+	–	–	–	–	–	+	–	–	–	+				
CSIRO	+	+	–	+	+	+	+	–	–	–	+	+	+	+	+	–	+	+	+	+	+	+	+	–	+	+
CSU	+	+	+	+	+	+	+	+	+	+	+	+	+	+	+	–	+	+	–	–	+	+	+	+	–	–
DNM	–	–	–	–	+	+	+	–	–	+	–	–	+	+	–	–	–	+	–	–	–	–	+	+	–	+
DERF	–	–	–	–	+	+	–	–	–	–	–	–	–	+	–	–	–	–	–	–	–	–	–	–		
ECMWF	+	+	+	+	+	+	+	+	+	+	+	+	+	+	+	+	+	+	+	+	+	+				
GFDL	–	–	–	–	–	–	+	–	–	–	+	–	–	+	–	–	–	–	+	–	–	–				
GISS	–	+	+	+	+	+	+	–	–	–	+	+	–	+	–	+	+	–	+	–	–	–				
GLA	+	+	–	+	+	+	+	–	–	+	+	+	–	–	–	–	+	–	–	–	–	–	–	–	+	+
GSFC	+	+	+	–	+	+	+	+	+	+	+	–	+	+	+	–	+	+	–	–	–	+	+	+	+	+
IAP	–	+	–	–	+	–	–	+	–	–	–	+	–	+	–	–	–	+	–	–	+	–			+	+
JMA	–	+	+	+	+	+	–	+	+	+	–	+	+	+	+	+	–	+	+	–	+	+	+	+	+	+
LMD	+	+	+	+	+	+	+	+	+	+	+	+	+	+	+	–	+	+	+	–	+	+	+	+		
MGO	+	+	+	+	+	+	+	+	+	+	+	+	+	+	+	–	+	+	–	–	+	+	+	+		
MPI	–	–	–	–	–	+	+	–	–	–	–	+	–	–	–	–	–	–	–	–	–	–	–	+	–	+
MRI	+	+	+	+	+	+	+	+	+	+	+	+	+	+	+	+	–	+	–	–	+	+	+	–	+	–
NCAR	+	+	+	+	+	+	+	–	–	+	+	+	–	+	+	+	–	–	–	–	–	–	–	+	–	–
NMC	+	+	–	+	–	+	+	+	–	+	+	+	+	+	+	–	–	–	–	–	–	–				
NRL	–	–	–	–	–	–	–	–	–	–	–	–	–	–	–	–	–	–	–	–	–	–				
RPN	+	+	+	–	–	+	–	+	+	+	–	–	–	–	+	–	–	–	–	–	–	+	–	–		
SUNYA	–	–	–	+	+	–	+	+	+	+	–	–	–	+	–	–	–	–	–	–	–	–	+	–	+	–
SUNYA/NCAR	–	–	–	+	+	–	+	+	+	+	–	–	–	+	–	–	–	–	–	–	–	–				
UCLA	–	+	+	+	+	–	–	+	+	+	–	–	–	+	+	+	–	+	–	–	–	–				
UGAMP	+	+	+	+	+	+	+	+	+	+	–	–	+	+	+	–	–	+	–	–	–	–	–	–	+	+
UIUC	–	+	–	+	–	+	+	+	–	–	+	+	+	+	–	+	–	+	–	–	–	–	–	+	–	–
UKMO	+	+	+	+	+	+	+	+	–	+	+	+	–	+	–	+	+	+	+	–	+	+	–	–	–	–
YONU	–	+	–	+	+	+	+	–	–	+	+	+	+	+	+	+	+	–	+	+	+	+	+	–	+	+
	1	2	3	4	5	6	7	8	9	10	11	12	13	14	15	16	17	18	19	20	21	22	23	24	25	26

Here + denotes active participation, while – denotes data availability only.

Reports from AMIP Diagnostic Subprojects

In this Newsletter we begin the presentation of brief reports from the AMIP Diagnostic Subprojects, selected from the summaries submitted in response to the request made in mid-1994.

Tropical Variability

Subproject No. 1: J. Slingo

The first phase of this subproject, whose purpose was to examine the ability of the participating models to simulate the tropical intraseasonal oscillation, is almost complete. Fourteen modeling groups were able to provide the requested time series of equatorial upper tropospheric velocity potential and zonal wind. These data have been analyzed using a variety of techniques such as time filtering and space-time spectral analysis to identify eastward and westward moving waves. The results have been compared with an identical assessment of ECMWF analyses for the period 1982–1991.

The models display a wide range of skill in simulating the intraseasonal oscillation. Most models show evidence of an eastward propagating anomaly in the velocity potential field, although in some models there is a greater tendency for a standing oscillation, and in one or two models the field is rather chaotic with no preferred direction of propagation. Where a model has a clear eastward propagating signal, typical periodicities seem quite reasonable although there is a tendency for the models to simulate shorter periods than in the ECMWF analyses where it is near 50 days. The results of the space-time spectral analysis have shown that none of the models produce spectra which compare well with the results from the ECMWF analyses. Several models have peaks at intraseasonal time scales, but nearly all have relatively more power at higher frequencies (<30 days) than the analyses. Most models also underestimate the strength of the intraseasonal variability.

The relationship between a model's intraseasonal activity, its seasonal cycle and the characteristics of its basic climate have been examined. It is clear that those models with weak intraseasonal activity also tend to have a weak seasonal cycle. It is becoming increasingly evident that an accurate description of the basic climate may be a prerequisite for producing a realistic intraseasonal oscillation. A preliminary report describing these results was circulated to participants earlier in the year, and a more comprehensive paper for publication as a WCRP Report has been submitted.

Low Frequency Variability

Subproject No. 2: F.W. Zwiers

The purpose of this subproject is to intercompare simulated and observed variability, primarily by means of a *potential predictability* calculation. Ordinary calculations of this sort use a one-way time-domain analysis of variance (ANOVA) to compare the total interannual variability of a seasonal or monthly mean with the component of variation in this mean which is induced by daily weather noise. In the AMIP context, in which many runs are available, a 2-way ANOVA is used to partition interannual variability according to source (initial conditions or model bias, external (i.e., boundary) forcing, internal sources and weather noise).

Work to date has consisted of methodological development and its application to observations and to an ensemble of 6 AMIP simulations which have been conducted in-house with the CCC GCM. The methodological development focused on finding ways in which to conduct the potential predictability calculation utilizing monthly means from the standard AMIP dataset rather than the daily data which was used formerly. This was necessary to reduce the volume of data required for analysis and to broaden the number AMIP simulations that can be analyzed. This work is now complete and we have begun transferring data from PCMDI to Victoria. Our intention is to prepare a standard set of variability diagnostics from each simulation and to subsequently involve participants by asking for their assistance with interpretation.

Figure 1 displays the zonally averaged interannual variance of DJF mean 500 hPa geopotential as computed from observations. Note the peak at the north pole (which may be due to sampling variability), a peak at about 75° N which is due to variation over Greenland, and a third peak at about 42° N which reflects the mid-latitude NH storm tracks.

Figure 2 displays locations at which the interannual variance of 500 hPa geopotential is significantly greater than the variance induced by weather noise alone. Significantly large varianceratios can be seen in a broad tropical band which presumably reflects slow variations in SST in the tropics. Also, note the significant ratios in the region of the Aleutian low, over the southwestern US and Mexico, and a suggestion that variations in the SPCZ are potentially predictable. These findings are in general agreement with those of Madden (1976) who used 1899–1972 NH MSLP station data, but are somewhat at odds with those of Trenberth (1985) who used 1972–80 ECMWF analyses and found significantly large ratios over Antarctica as well as in the tropics.

Figure 3 displays the zonally averaged interannual variance of DJF mean 500 hPa geopotential aggregated across the 6 AMIP simulations. Note that the simulated variance is only about 50% of that observed. This discrepancy is larger than that which can be attributed to sampling variation (in the observations), observational error, analysis error or the effects of network and analysis system changes during the 10-year AMIP period. The peak at the north pole is not present in the simulations, the peak at 75° N which is associated with variation over Greenland is present (but not large enough), while the peak associated with northern mid-latitude storm tracks is entirely absent. Centers of variation which are associate with these storm tracks are present in the simulated climate but are much weaker than observed. Variation in the tropics is also only about 50% of that which is observed despite the imposition of the observed SSTs at the lower boundary.

Application of the 2-way time-domain ANOVA reveals that there are no significant contributions to the total simulated interannual variability of 500 hPa height from either the initial conditions or from sources internal to the model. However, there are significant contributions from boundary forcing. This contrasts strongly with Zwiers (1987) who found potential predictability in a 20-year simulation with CCC GCMI from sources apparently internal to that model. When the 2-way ANOVA computation is repeated with 850 hPa temperature we find strong contributions from boundary forcing and weak evidence that slow land surface variations (which are internal to the model) have a local potentially predictable effect over tropical land masses.

Figure 4 displays the result of the test for potential predictability from external sources for 500 hPa geopotential. The tropical band of large variance ratios is wider than in the observations, partly because the larger volume of data has increased the sensitivity of the test and partly because the simulated climate contains less weather noise than the observed climate. Note also the centers located over the north-eastern Pacific and eastern North America which are felt to reflect the simulated atmosphere's response to ENSO, a suggestion that variations in the simulated SPCZ are boundary forced and, consistent with Trenberth (1985), a suggestion that variations at high southern latitudes are potentially predictable.

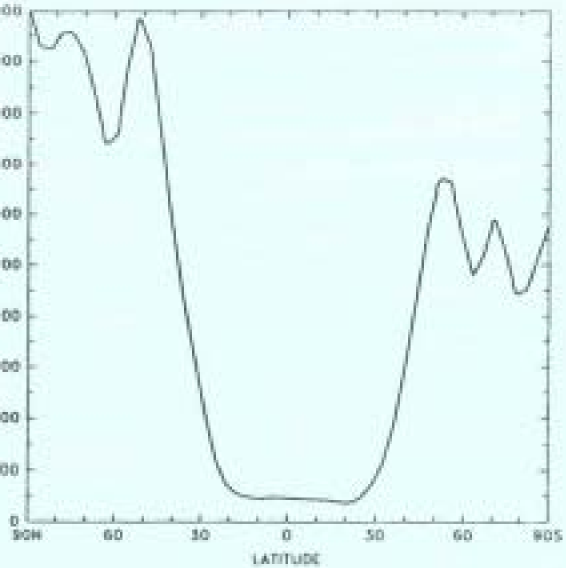

Fig. 1. Zonally averaged interannual variance in $(gpm)^2$ of DJF mean 500 hPa geopotential computed from 1979–88 NMC analyses.

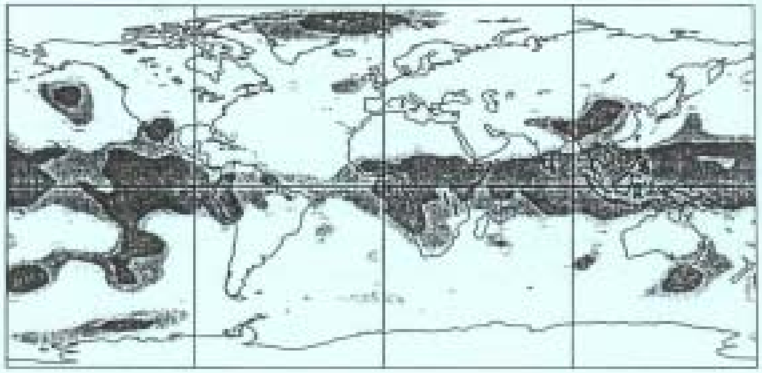

Fig. 2. The significance of the ratio of the interannual variance of DJF mean 500 hPa geopotential to the weather-noise induced variance of DJF mean 500 hPa geopotential (see Zwiers, 1987 for details). The light, medium and dark shading indicate ratios that are greater than one at the 10%, 2% and 0.4% significance level, respectively.

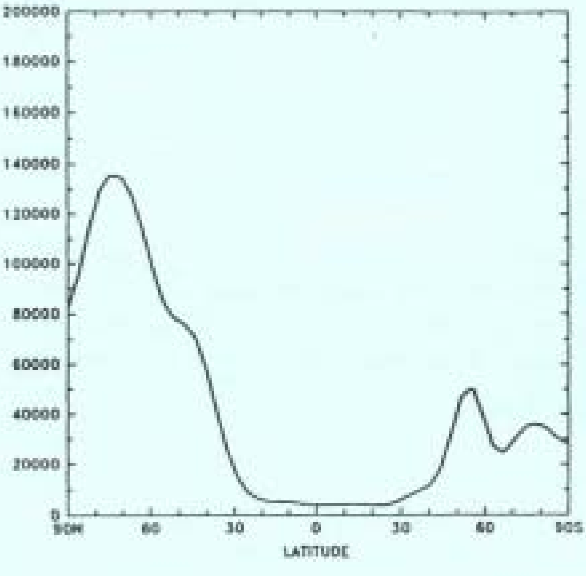

Fig. 3. As in Fig. 1, except for DJF mean 500 hPa geopotential simulated in the ensemble of 6 CCC GCMII AMIP runs.

Fig. 4. As in Fig. 2, except that the variance ratio diagnoses the external boundary forcing contribution to the interannual variance simulated by the CCC GCMII in an ensemble of 6 AMIP runs.

Surface Ocean Fluxes

Subproject No. 5: D. Randall and P. Gleckler

We are investigating energy fluxes across the surface of the ocean, and the implied ocean energy transports as simulated by the atmospheric general circulation models participating in AMIP. Of course, in all of these models ocean surface temperatures and sea-ice boundaries are prescribed. The ocean meridional heat transport that would be required to compensate for these surface fluxes has been computed from the ten-year means of the surface fluxes. Our analysis to date shows that the implied ocean energy transports are critically sensitive to the radiative effects of clouds, to the extent that even the sign of the Southern Hemisphere ocean energy transport can be affected by the errors in simulated cloud-radiation interactions.

There is no need to identify the models because the point to be made applies to all of them, and is illustrated in the accompanying figure. The upper panel of the figure shows the ocean energy transports inferred directly from the simulated net surface energy fluxes produced by each model (after removing the generally small global mean). The lower panel shows the corresponding results obtained if the atmospheric energy transport simulated by each model is subtracted from the total (atmosphere plus ocean) energy transport inferred from ERBE (Earth Radiation Budget Experiment) data. In effect, the lower panel shows the ocean energy transports that would be implied by each atmospheric model if the simulated Earth radiation budget was perfect and the atmospheric energy transports were unchanged.

In the upper panel of Fig. 5 the ocean energy transports implied by many of the models are northward at all latitudes, even in the Southern Hemisphere. In the lower panel, the "ERBE-corrected" ocean energy transports are poleward in both hemispheres for all models. The difference between the two panels is quite striking, and shows that errors in the simulated Earth radiation budget are responsible for the presumably erroneous northward ocean energy transports in the Southern Hemisphere, as produced by several of the models. The errors in the simulated Earth radiation budgets are likely due to errors in the distribution of clouds and/or the cloud optical properties.

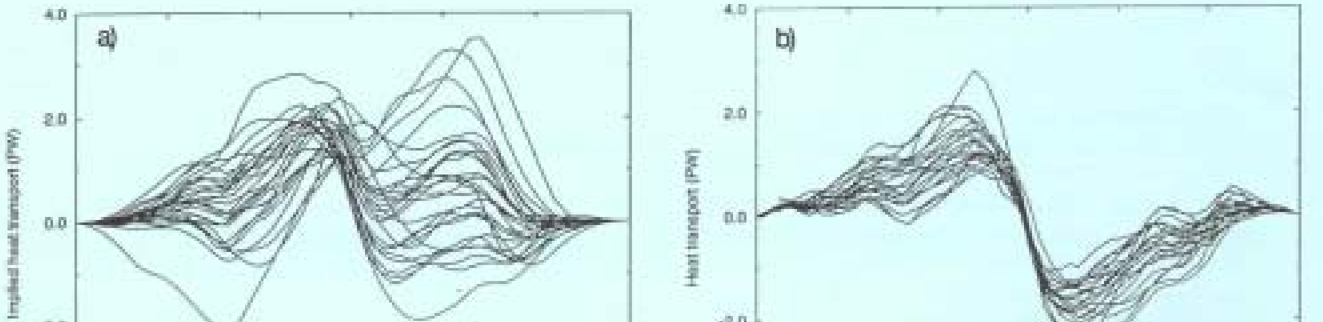

Fig. 5. Panel (a) shows the annual mean global northward ocean energy transport implied by the AMIP simulations. Panel (b) shows the corresponding implied ocean energy transport if the simulated atmospheric energy transport produced by each model is subtracted from the total (ocean plus atmosphere) energy transport implied by ERBE data.

Monsoons

Subproject No. 6: K.R. Sperber and T.N. Palmer

As part of the charge of the AMIP subproject "Monsoons" we have been evaluating the ability of the models to simulate regional precipitation variations. Here we report on interannual rainfall variations simulated over the Indian subcontinent averaged over the months June-July-August-September, and over the Nordeste region of Brazil averaged over the months March-April-May. For each model the rainfall index has been normalized by removing its mean and dividing by its standard deviation. When compared with the observed all-India rainfall index of Parthasarathy *et al.* (1992), the heavy black curve in Fig. 6a, the indices exhibit little or no coherence among the simulations in representing the observed interannual variations of Indian monsoon rainfall, even during 1987 and 1988 when the large SST anomalies associated with El Niño and La Niña provided a substantial perturbation to the tropical flow. A similar analysis of the simulated March-April-May Nordeste precipitation and March-April observations (Hastenrath 1992, personal communication) is given in Fig. 6b. While there is still significant spread among the models, there is some indication of qualitatively coherent behavior, particularly from 1982–88.

In an effort to find some underlying order in the ability to represent precipitation variations through the use of teleconnection studies, we perform lag 0 correlations of each model's rainfall indices with the SST. Only those models that qualitatively represent the observed teleconnection pattern are retained in Figs. 6c–d. With regard to the all-India/SST relationship, 17 of the models have shown some skill at representing the observed teleconnection pattern. These models all qualitatively represented the relative increase in precipitation in 1988 relative to 1987. Although 1982 and 1983 were also dry and wet years, analogous to 1987 and 1988, the "universal" coherency exhibited by this reduced set in the rainfall anomaly tendency from 1987 to 1988 is not found in 1982 and 1983. Either the models lack the necessary sensitivity for the Indian monsoon precipitation to respond to the 1982 and 1983 SST, or other less well understood controlling factors, such as Tibetan snowcover, soil moisture or extratropical influences play a significant role in modulating the interannual variations of the Indian monsoon.

For Nordeste, only 6 of the models were unable to qualitatively represent the observed teleconnection pattern. With their exclusion, the reduced set of indices (Fig. 6d) exhibit a decrease in the spread, particularly during the later portion of the integrations. Given the intimate relationship of Nordeste rainfall to tropical SSTs (Hastenrath 1990, Ward and Folland 1991, Sperber and Hameed 1992), stronger than the Indian monsoon/SST relationship, the Nordeste variations are inherently more predictable than those associated with the Indian monsoon. This is borne out from the analysis of these rainfall indices from ensemble AMIP integrations with the ECMWF model, presented in Figs. 6e-f. These ensembles differed only in their specification of initial conditions. For the Nordeste region, Fig. 6f, the surface forcing dominates over the internal atmospheric variability, whereas in the case of the Indian monsoon rainfall variations, Fig. 6e, the initial conditions exert a strong influence through random or chaotic atmospheric perturbations. In this case the 1987–1988 Indian monsoon tendency is robust owing to the strong SST anomalies that persisted into JJAS. At most other times there is little or no agreement among the realizations with regard to the sign of the anomalies or their tendency.

The use of a regional rainfall index as a means of model verification has proven to be a stringent test of a model's ability to simulate interannual variations. With regard to the influence of the remote SST forcing, nearly half of the models evaluated exhibited fundamental difficulties by their failure to even realize the correct phase of the observed all-India rainfall/SST teleconnection. We find that the link between Indian monsoon rainfall and SST is strongest under ENSO conditions, particularly when substantial anomalies in the tropical Pacific Ocean persist during June-September. At other times little or no consensus among the simulations exists with regard to Indian monsoon rainfall, even in the initial condition sensitivity simulations performed with the ECMWF model. Contrary to this, the simulations of Nordeste rainfall variations are more coherent owing to fact that their dominant controlling factor is tropical SST and from their relative insensitivity to initial conditions.

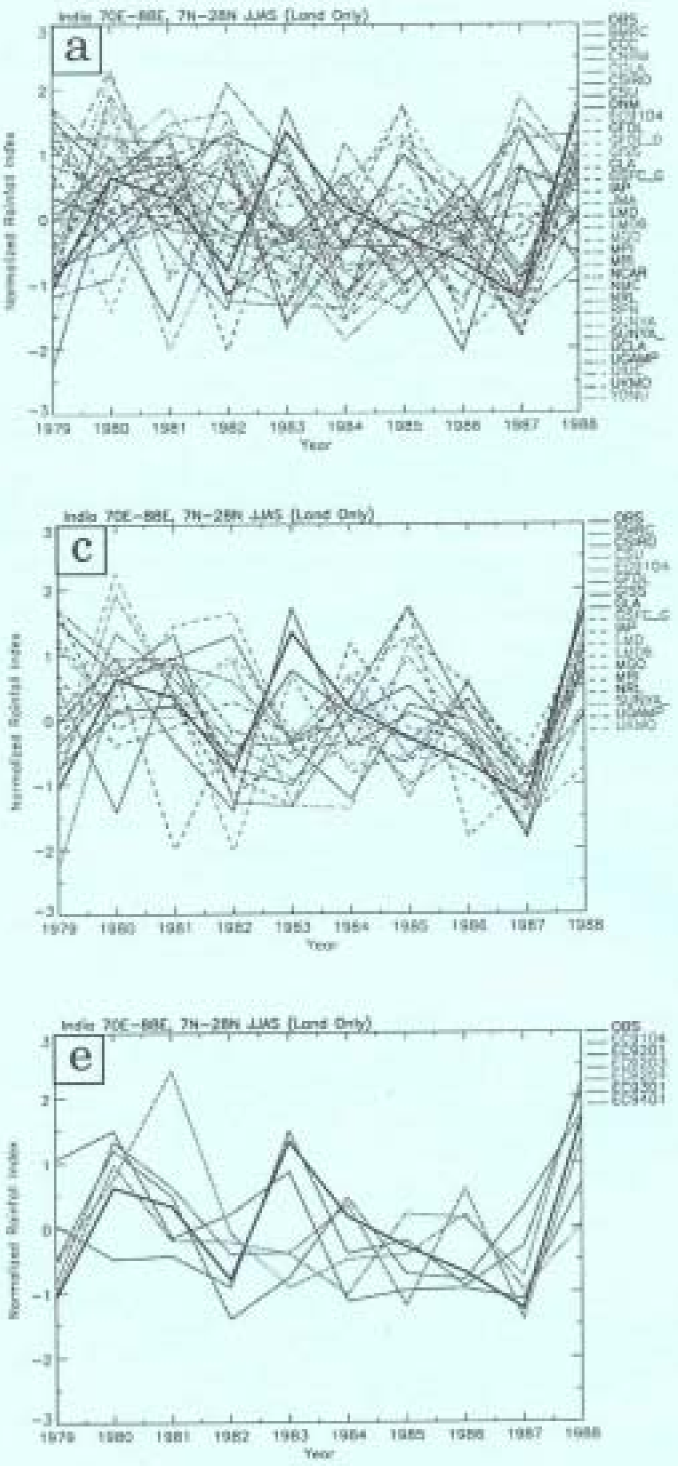

Fig. 6. a) June–July–August–September averaged all-India rainfall indices for the period 1979–88 for selected AMIP models; b) March–April–May averaged Nordeste rainfall indices for the period 1979–88 for selected AMIP models; c) same as (a) except for those models that have qualitatively simulated the observed rainfall/ENSO teleconnection; d) same as (b) except for those models that have qualitatively simulated the observed rainfall/ENSO/tropical Atlantic teleconnection; e) all-India rainfall indices from an ensemble of initial condition AMIP integrations with the ECMWF model; f) Nordeste rainfall indices from an ensemble of initial condition AMIP integrations with the ECMWF model.

Hydrologic Processes

Subproject No. 7: W.K.-M. Lau, Y.C. Sud and J.H. Kim

The objective of this subproject is to evaluate the ability of GCMs to simulate the global hydrologic cycle and to explore means of validation of GCM precipitation and hydrologic processes with space- and ground-based observations. We have completed the intercomparison of the precipitation (P), evaporation (E) and surface hydrologic forcing (P–E) for 13 AMIP GCMs and for relevant observations over a variety of spatial and temporal scales. These include global and hemispheric means, latitudinal profiles, selected areal means for the tropics and extratropics, and for ocean and land. Over land, the GCM runoff is also compared to runoff estimates from river-routing models and from hydrographic data. In addition, we have computed pattern correlations among models and observations as a function of the calendar months, harmonic dials for annual and semi-annual cycles, and rain-rate frequency distributions.

As expected, the results are mixed. Except for a few outliers, the models produce a global and hemispheric mean annual hydrologic cycle to within approximately 20–30% of that observed. The differences among model precipitation estimates over the ocean are as large as those among climatological estimates. The discrepancies among models are largest over the land regions. These may be due to the diverse landsurface schemes used in the different models. As a whole, the models seem to follow the simple "rule of thumb" that more (less) rain is associated with a cooler (warmer) land surface (as shown in Fig. 7). We also found that not all the AMIP GCMs have a globally balanced water cycle over the 10-year AMIP integration, particularly models from numerical forecast centers where presumably no special attention was devoted to conserving the water cycle over a long-term integration.

Another noteworthy result is the intercomparison of ensemble mean rainfall frequency distribution. A common feature shared by the AMIP models is that they all underestimate the precipitation in the light rain (0–1 mm/day) category. The ratio between the lowest rainrate and the next (1–2 mm/day) category for the model ensemble average is approximately 1 to 0.8. In contrast, the same ratio from observations is approximately 1 to 0.4. The models overestimate the rainrate in the medium rain category (2–4 mm/day) by about 15–20% compared to observations, while at higher rainrates, the models are consistent with observation. These findings imply that there is a reasonable degree of realism in the model parameterization of convective rain, but that there may be a fundamental problem regarding the production of light rain. This may be due to the improper treatment of shallow convection, in particular boundary-layer stratus, in most GCMS.

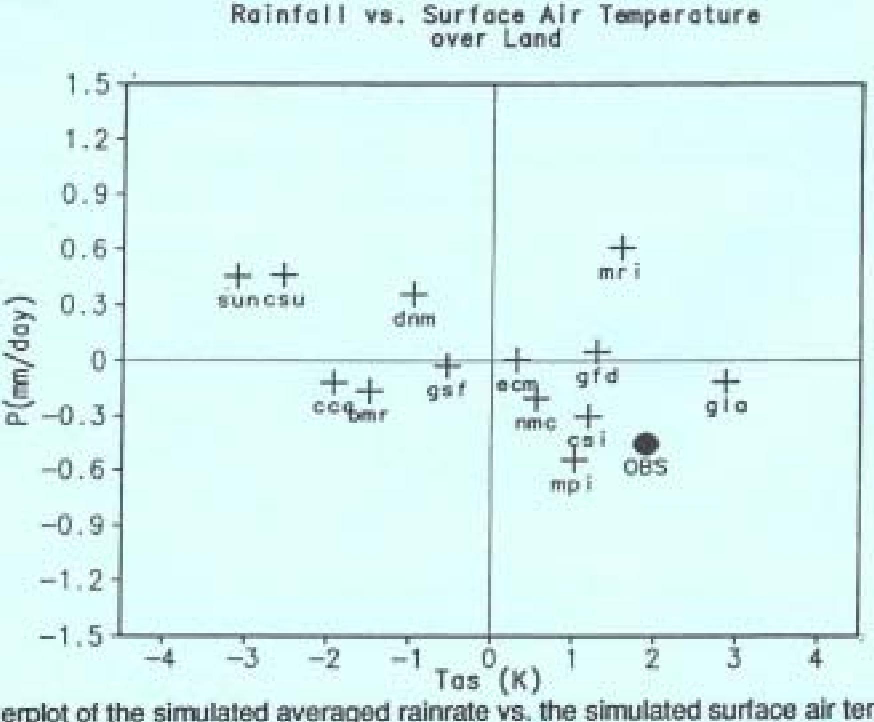

Fig. 7. Scatterplot of the simulated averaged rainrate vs. the simulated surface air temperature during 1979–1988 over land. The observed data are from the climatology of Legates and Willmott. Regions with land ice are excluded.

Southern Hemisphere Circulation

Subproject No. 9: B. McAvaney

Twenty of the AMIP model simulations have been systematically compared for a number of features of the Southern Hemisphere circulation. Thus far emphasis has been restricted to the simulations of mean sea-level pressure (MSLP), temperature and winds. Intercomparisons have been made of *(i)* seasonal variation in the amplitude and latitude of the circumpolar trough in each ocean basin, *(ii)* spatial variation in the amplitude and phase of the semi-annual oscillation in MSLP, *(iii)* frequency of occurrence of the split jet at 200 hPa in winter in the Australasian sector, *(iv)* rms error in zonal mean and long wave MSLP fields, and *(v)* the semi-annual oscillation in temperature gradient and its relationship to pressure changes in the circumpolar trough. This latter feature is shown in Fig. 8. A number of the models reproduce the observed amplitude of the semi-annual component in the pressure in the trough (about 2 hPa), but the amplitudes of the semi-annual component of temperature gradient are all somewhat weaker than the observed value of about 1.3K. The model simulations show a strong linear relationship between these quantities.

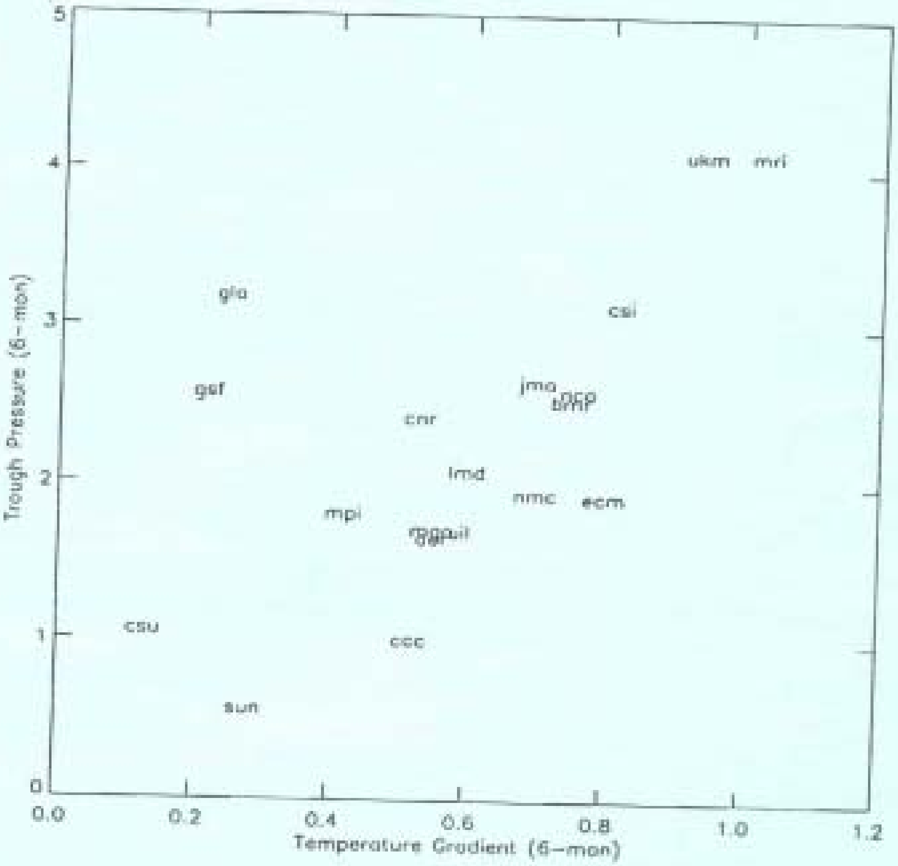

Fig. 8. The amplitude of the semi-annual component of the pressure (hPa) in the circumpolar trough versus the amplitude of the semi-annual component of the temperature gradient (K) between 50 S–65 S at 500 hPa as simulated by 20 AMIP models (identified by the first three letters of their official acronym; see page 5).

Landsurface Processes

Subproject No. 12: P.K. Love and A. Henderson-Sellers

This subproject is Phase 3 of the GEWEX Project for Intercomparison of Landsurface Parameterization Schemes (PILPS), and is examining AMIP models that have a connection with PILPS. Three stages have been identified for the AMIP-related research. The first, which has been completed in the form of a technical report, examines the general landsurface climatologies and identifies regions for study based on areas of model consistencies and differences in forcing and response variables. The second stage, which is near completion, examines regions used in the first stage and the regions selected for the PILPS off-line simulations. The third stage is comparing the output from AMIP AGCMs that have completed simulations with two different landsurface schemes.

One of the interesting results from the first stage has been the large landsurface energy residuals. These are defined as the sum of latent heat, sensible heat and net radiation. Of the seven AMIP models examined, the global surface energy budget was found to be unbalanced for three models. Two models had a global energy residual of a magnitude of about 6 Wm^{-2} and one model had a residual of 13 Wm^{-2}. These residuals were not simply associated with high latitudes, but generally occurred significantly at all latitudes (Fig. 9). The residuals do not appear to be related to initialization, and similar global values were found using only grid-points without snow cover. If the energy residuals are not due to errors in model coding and in the processing of the model output, they must be artifacts of the land surface parameterization. Some landsurface schemes fix the temperature of their deepest soil layer and if this temperature is not equal to the average of the scheme's surface temperature, then there will be a net flux into or out of the soil. This has been proposed by one group as the explanation for their energy residuals. The models that do not use a fixed deep-layer temperature employ methods that use zero flux formulations in which there is no heat transfer at the deepest soil layer. As these models do not allow heat transfer at their lower boundary, energy cannot be lost from the soil except through the surface. Two of the models with high energy residuals employ such schemes, as do three of those with low energy residual. The energy residuals are being studied in more detail in the second and third stages of the subproject.

Queries with regard to the PILPS off-line experiments can be sent by e-mail to pilps and queries specifically related to PILPS Phase 3 (AMIP Diagnostic Subproject 12) can be sent to pklove, both @ mqmet.cic.mq.edu.au

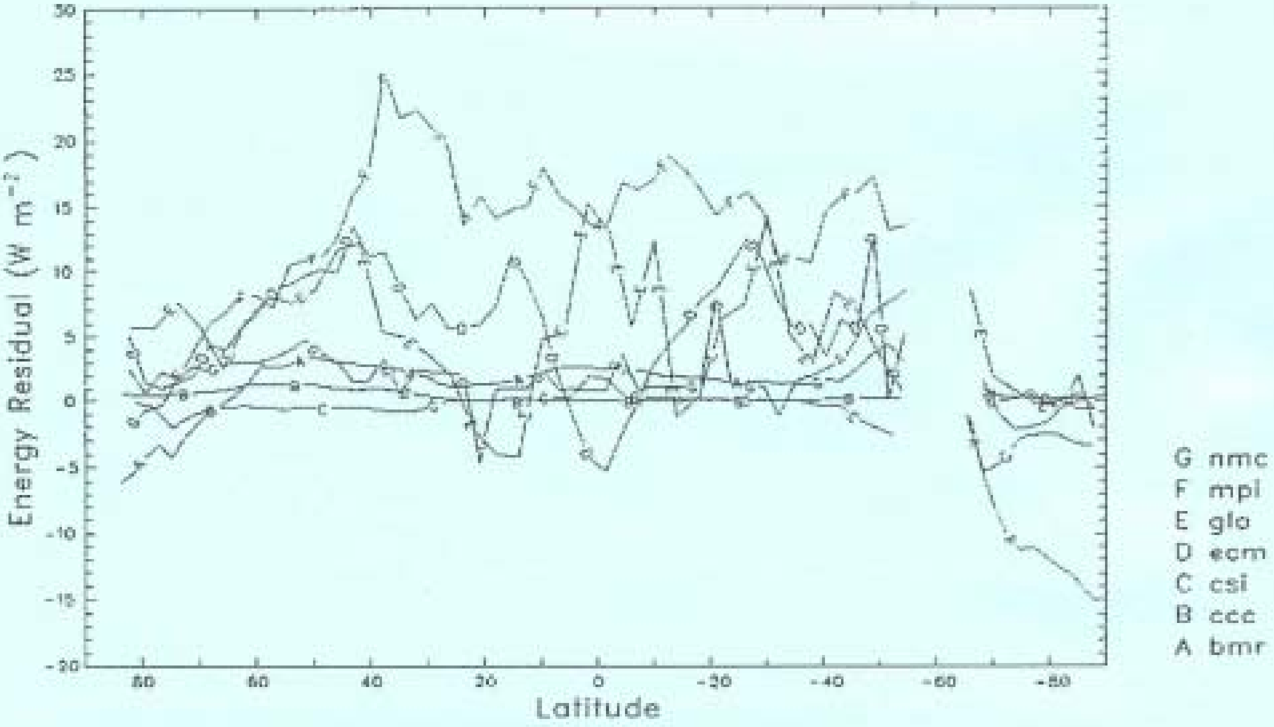

Fig. 9. Annually averaged zonal energy residual over land in selected AMIP models.

Cloud-Radiative Forcing

Subproject No. 14: G.L. Potter

As a first step in the diagnosis of net cloud-radiative forcing from the AMIP standard output, the ten-year zonal average net cloud forcing for both January and July was compared to the ERBE S4 product for the four ERBE years 1985–1988. The zonal average DJF cloud radiative forcing is shown in Fig. 10. The results indicate a systematic error among all models compared to ERBE: In both DJF and JJA (not shown) and from approximately 30° N to 30° S the models produce excessive negative cloud forcing. That is to say, the models' clouds are too effective in cooling the Earth. In the high latitudes of the summer hemisphere the opposite error is present. With the limited amount of shortwave and longwave flux data available (which were unfortunately not explicitly included in the AMIP standard output), it was determined that this error in the topics is almost entirely explained by errors in the shortwave cloud radiative forcing, while the error in the high latitudes is likely due to the underprediction of cloud cover. In the tropics, there is some suggestion from surface flux data that the Earth's surface is absorbing too much solar radiation. In conjunction with the excessive reflection to space, the only reasonable conclusion is that the models' atmospheres are not absorbing enough solar radiation. These conclusions were independently reached by Cess and Ramanathan. If substantiated by additional surface measurements, this systematic error suggests that virtually all atmospheric GCMs in use today substantially underestimate the shortwave absorption by the atmosphere in the tropical latitudes. If atmospheric models are used in their present form to couple to ocean models, it is apparent that large errors in the simulated poleward energy transport could occur for this reason alone.

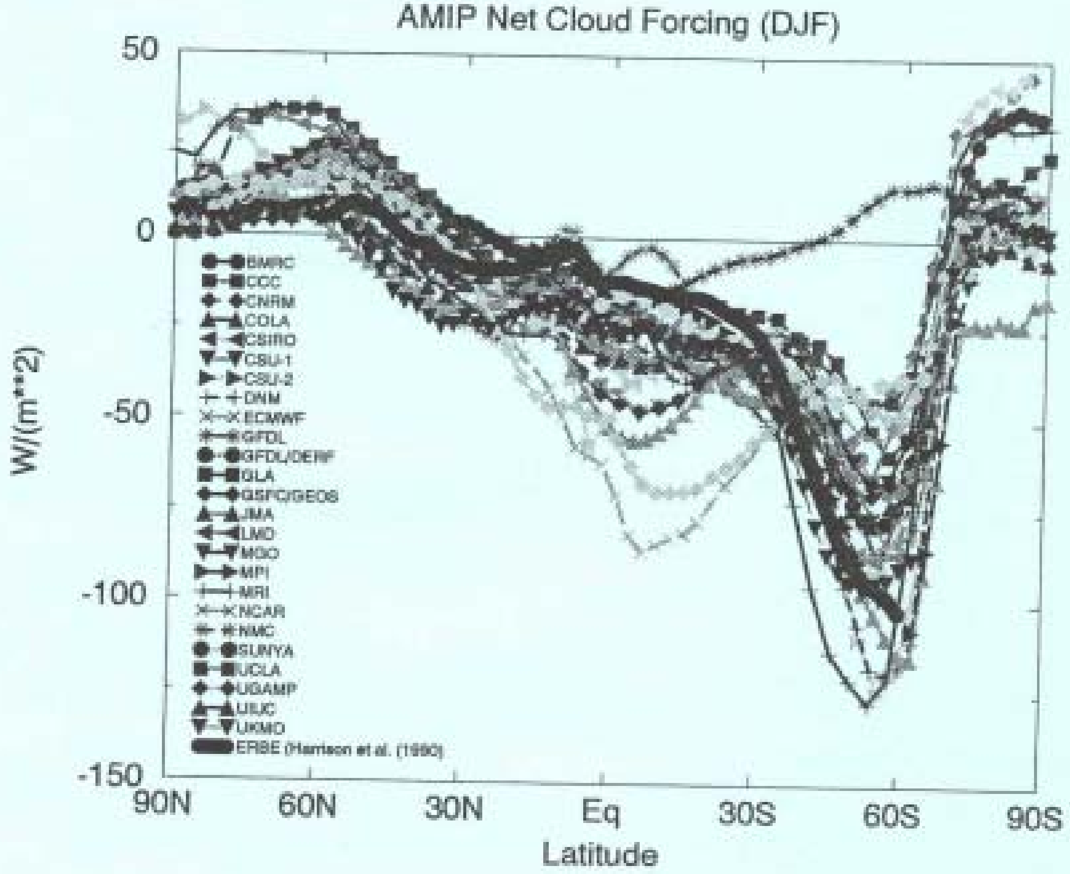

Fig. 10. The December, January and February zonal average net cloud radiative forcing from 25 AMIP models, and from observations of the Earth Radiation Budget Experiment (ERBE) during 1985–1988.

Angular Momentum

Subproject No. 15: R. Hide, J.O. Dickey, S.L. Markus, R.D. Rosen and D.A. Salstein

The principal objective of this subproject is to examine the ability of the AMIP models to represent satisfactorily temporal fluctuations in (1) all three components of the angular momentum of the whole atmosphere on interannual, seasonal, and shorter time scales, and (2) concomitant torques associated both with surface friction in the oceanic and continental boundary layers and with pressure gradient forces across topography. The atmospheric angular momentum (AAM) vector consists of the axial and two equatorial components, and its variations are related to small but measurable changes in the Earth's rotation. By elementary dynamical reasoning, AAM fluctuations must be intimately linked as well with global energetic interactions.

We have begun by intercomparing time series of seasonal and interannual variations in the axial component of AAM based on the AMIP data available, which, by early 1994, consisted of monthly mean values from 12 models. Also being utilized are observed momentum values calculated from monthly means of National Meteorological Center (NMC) global wind analyses, and geodetic data on length-of-day fluctuations. If the first intercomparisons are typical, most of the models represent the global mean value of the axial component of AAM satisfactorily, but they generally exhibit significant discrepancies on a regional basis. Seasonal and interannual variations of the AAM signal are represented with varying degrees of accuracy, with the best models simulating major aspects of the variations seen during the two El Niño events that occurred during the AMIP period (Fig. 11). While considerable variability is found in the latitudinal structure of the AAM response among the models, the ensemble mean exhibits clear evidence of poleward propagation on interannual time scales, similar to a pattern found in latitudinally-belted AAM data derived from NMC analyses (not shown).

When more complete AMIP data become available, we will analyze and intercompare the ability of selected models (on the basis of their performance on seasonal and interannual time scales) to reproduce the observed angular momentum fluctuations on intraseasonal time scales. To date, results of the subproject have been presented at the 1993 Fall Meeting of the American Geophysical Union and at the American Meteorological Society's Sixth Conference on Climate Variations in 1994.

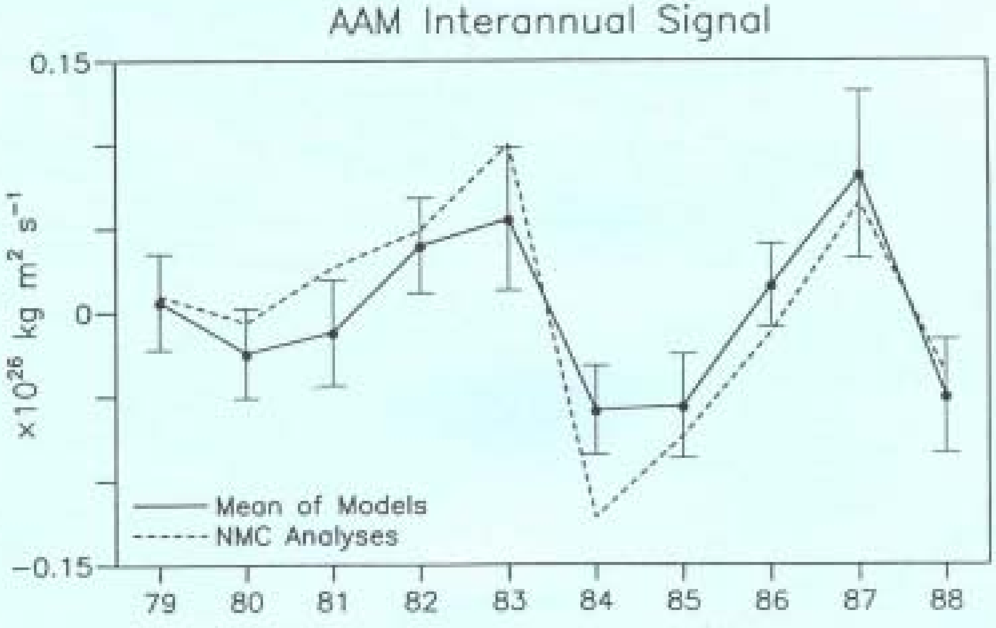

Fig. 11. The average interannual anomaly of relative axial atmospheric angular momentum, computed by integrating zonal winds over the globe between 1000 and 50 hPa of twelve AMIP models for each calendar year of the decade 1979–88 (solid line). The value for ± one standard deviation of the twelve model values for each year is represented by the vertical bars. The dashed line indicates the observed (NMC) annual values. The decadal mean of the series for each model and for NMC has been subtracted in performing the calculations.

MSU Temperature

Subproject No. 19: J.R. Christy

The objective of this subproject is to utilize the high-precision satellite Microwave Sounding Unit (MSU) measurements of atmospheric temperature as a base for validation and study of output from global climate models participating in AMIP. Comparisons of the model output (850–200 hPa thickness) with the MSU tropospheric temperature have been performed.

We have found that the global mean thickness anomalies of the models, once normalized by the SST forcing, vary from 40 m per degree of SST change to 65 m per degree, vs. the observed value of 55. In addition, the decadal trends of the tropospheric temperature (derived from the thickness anomalies) are all positive over the ten-year period, and 11 of the 13 models produced trends greater than the +0.11 deg/decade forcing provided by the SST. The actual trend in the MSU was near zero. These results are displayed in Fig. 12 where models are arranged according to the sensitivity of the troposphere to SST forcing, with the decadal trend represented by the horizontal bar.

The global mean tropospheric temperature anomalies are reproduced fairly well, with correlations of annual anomalies (models vs. MSU) generally above 0.8. The ENSO events of 82–83 and 87 contribute the largest variance in both sets of data.

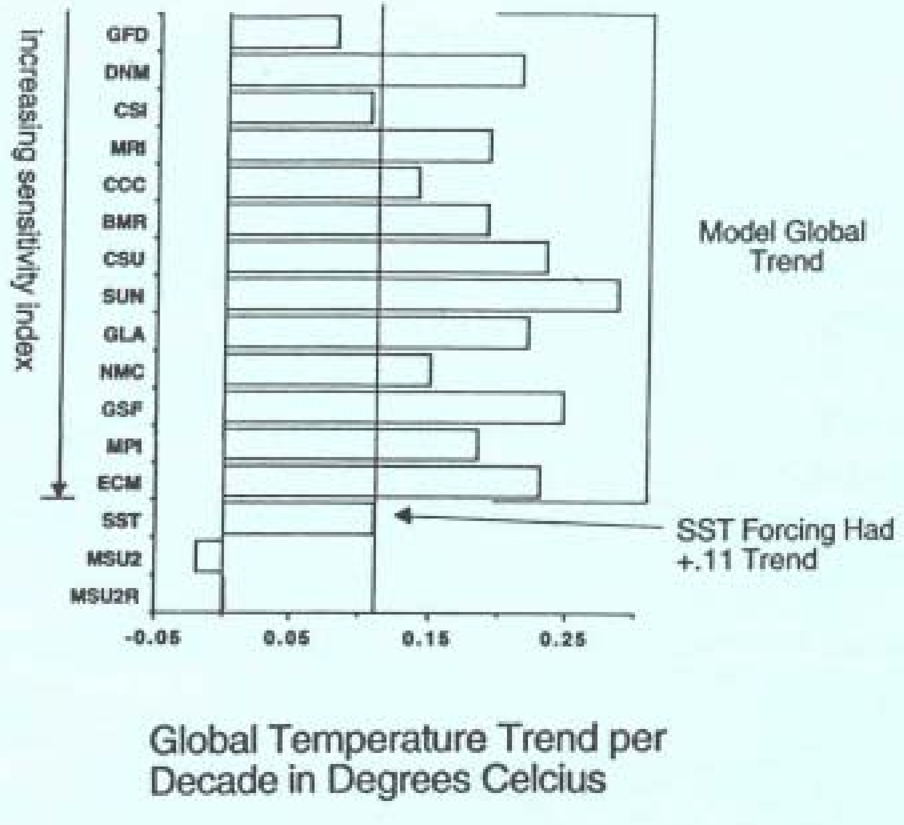

Fig. 12. 1979–88 trends in global mean tropospheric temperature for 13 global climate models in AMIP, as well as trends in the SST forcing, and two MSU layers (MSU 2R being the most appropriate for comparison).

Surface Climatologies

Subproject No. 21: G. Srinivasan, M. Hulme and C.G. Jones

The purpose of this subproject is to compare the AMIP models' simulation of monthly precipitation and temperature with corresponding land-based climatologies over the AMIP decade. Of these, precipitation is the more difficult to simulate. Monthly precipitation fields produced by a subset of 19 currently available AMIP model experiments have been evaluated for the tropical region using a land-only observed dataset for the period 1980–1988. The models show large variations in their ability to reproduce observed tropical precipitation, although spatial correlations indicate that some of the models simulate the pattern of the observed precipitation fairly well. The correlations are strongest during DJF and weakest during JJA, while the RMS errors of the models are largest during JJA (see Fig. 13). Individual models also exhibit a consistent dry or wet bias as compared to the observed precipitation fields.

Comparison between model and observed precipitation time series for two central Pacific locations show that most models are unable to reliably reproduce interannual precipitation variability in this region. The exceptions are the ECHAM, ECMWF and JMA models which simulate the observed precipitation characteristics of this region with a reasonable degree of fidelity as demonstrated by their high spatial, and relatively good anomaly, correlations. There is a clear tendency for better performance to be associated with higher resolution models.

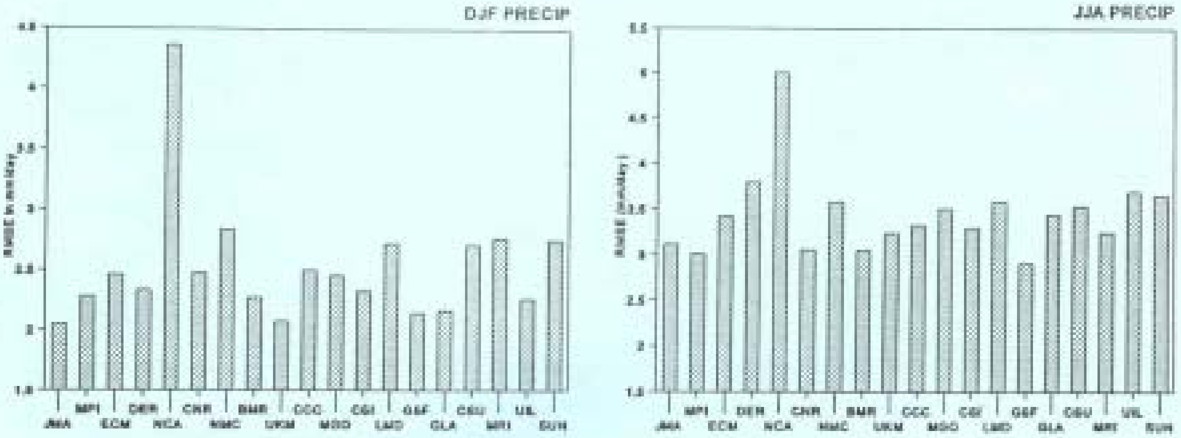

Fig. 13. Average (1980–1988) RMSE (in mm day^{-1}) of selected AMIP model precipitation fields for DJF and JJA as compared to the CRU0092 observed dataset.

Energetics

Subproject No. 22: H.L. Tanaka

The purpose of AMIP project has close connection to that of MECCA project. Therefore, many of AMIP investigators are also MECCA investigators. In this short report of the preliminary results, a comparison of the energy spectra in the zonal wavenumber domain is presented for NCAR/CCM2 and observation by the ECMWF. The analysis method is based on the standard spectral energetics by Saltzman. The energetics characteristics for the ECMWF global analysis are examined for consecutive 5 years from 1986 to 1990 to find the average energy levels as well as the interannual variability in the observed atmosphere. The objective of the present energetics analysis is to understand how the energy levels and energy interactions depend on the horizontal resolution of various climate models. For this reason, the energetics characteristics of the NCAR/CCM2 are compared for the resolutions of R15, T42, T63, and T106. Since the AMIP models have diversified model resolutions, a comprehensive comparison of the same model outputs for different horizontal resolution would offer a meaningful milestone for the diagnostic analyses.

Figure 14 illustrates kinetic and available potential energy spectra for various resolutions of the CCM2 during northern winter. Plotted also in the same figure is the 5 year mean energy level and the standard deviation for the ECMWF analyses. The characteristic energy spectra at the truncation wave number is clearly detectable. It is shown that the energy spectra for various model resolutions are within the deviation of the ECMWF analyses. The spectral energetics results are available for the complete energetics terms, such as baroclinic conversion, zonal-wave interactions, wave-wave interactions, generation, and dissipation.

As the AMIP diagnostic subproject, we plan to extend the present spectral energetics analysis for other AMIP models, including those of JMA, MRI, NMC and ECMWF.

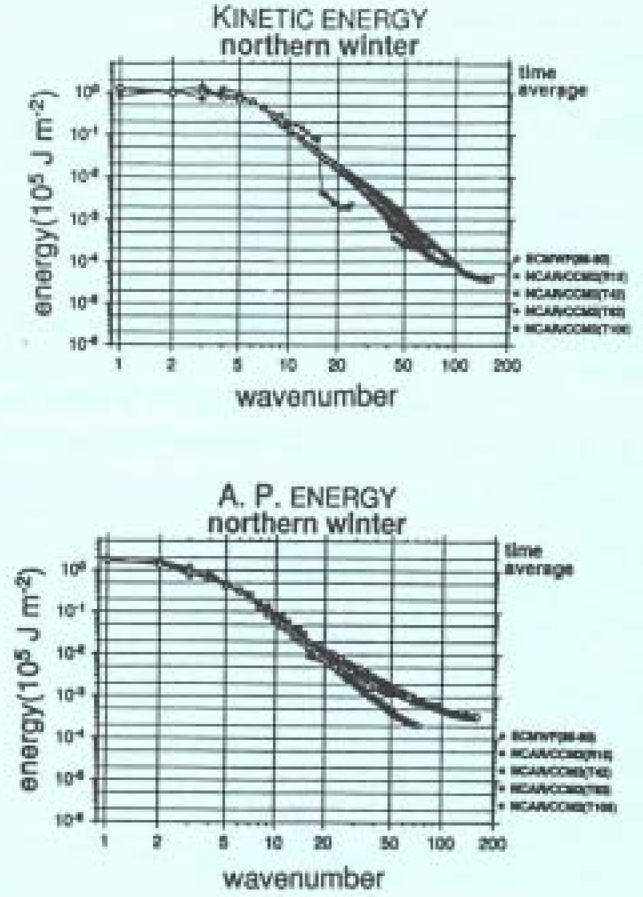

Fig. 14. The wavenumber spectra of kinetic energy and available potential energy as simulated by the NCAR CCM2 AMIP model at different resolutions in comparison with ECMWF analyses.

East Asian Climate

Subproject No. 25: W.-C. Wang, G.-X. Wu,
H.-H. Hsu, and X.-Z. Liang

This subproject sponsored a workshop on "General circulation model simulation of East Asian climate" during October 18–20, 1994 at the Atmospheric Sciences Research Center, State University of New York, University at Albany. The workshop was attended by fourteen scientists from five groups: Institute of Atmospheric Physics (IAP), Chinese Academy of Sciences; Department of Atmospheric Sciences, National Taiwan University (NTU); Atmospheric Sciences Research Center, State University of New York at Albany (SUNYA); National Climate Center, Chinese Meteorological Administration (CMA); Program for Climate Model Diagnosis and Intercomparison (PCMDI), Lawrence Livermore National Laboratory. Several graduate students from SUNYA also participated.

Prof. Wei-Chyung Wang gave a brief welcome and stated the objective of the workshop. He elaborated on three relevant questions to be addressed concerning the subproject: What are the observed characteristics of EAC? (e.g., the temporal and spatial variations of the monsoon), Can we quantify these characteristics so that they can be used to compare with GCM simulations? (e.g., the climatological mean evolution of the monsoon), and What can we say about the GCM if the model simulated characteristics "agree" with the observations? It is clear that understanding the mechanisms that influence the EAC is the ultimate goal of the subproject.

The workshop was organized around two sessions: The first session (one-day) consisted of presentations of GCM simulations and diagnoses of east Asian climate from the individual groups; the second session (two days) included discussion and writing of the workshop document for the planning of future research. For the eight presentations given in session 1, Drs. Michael Dudek and Art Samel served as reporters for the GCM simulation and GCM diagnostics, respectively. In the second session, Dr. Xin-Zhong Liang gave an overview of the important characteristics of EAC on various time and spatial scales; he also presented the SUNYA 1994–95 plan for the subproject. This was followed by presentations from Prof. Guo-Xiong Wu, Prof. Huang-Hsiung Hsu, Dr. K. Sperber and Dr. Yong Luo outlining, respectively, the IAP, NTU, PCMDI and CMA research for next year. All groups recognized the importance of examining the model's ability to simulate the climatological mean evolution of the east Asian monsoon and agreed to conduct such a joint task within the next six months and to present the preliminary results at the May 1995 AMIP conference. Data needed to conduct model-to-observation comparison were also discussed.

AMIP Contacts

Questions, suggestions and comments on AMIP are welcome, and may be directed to the following:

General

PCMDI role — Larry Gates
tel: (510) 422-7642
fax: (510) 422-7675
email: gates5@llnl.gov

WGNE AMIP Panel — Larry Gates, Chairman
George Boer (CCC, Victoria)
Lennart Bengtsson (MPI, Hamburg)
David Burridge (ECMWF, Reading)

WCRP role — Roger Newson (Geneva)

DOE role — Mike Riches (Washington, DC)

PCMDI technical support

Computer time, user accounts — Jerry Potter
tel: (510) 422-1832
fax: (510) 422-7675
email: potter@oliver.llnl.gov
or
Lisa Corsetti
tel: (510) 422-8705
fax: (510) 422-7675
email: lisa@zeppelin.llnl.gov

DRS and CDMS software — Bob Drach
tel: (510) 422-6512
fax: (510) 422-7675
email: drach@cricket.llnl.gov

VCS and DDI software — Dean Williams
tel: (510) 423-0145
fax: (510) 422-7675
email: williams@asia.llnl.gov
or
Bob Mobley
tel: (510) 422-7649
fax: (510) 422-7675
email: mobley@rabbit.llnl.gov

Validation data — Mike Fiorino
tel: (510) 423-8505
fax: (510) 422-7675
email: fiorino@typhoon.llnl.gov

Model documentation — Tom Phillips
tel: (510) 422-0072
fax: (510) 422-7675
email: phillips@tworks.llnl.gov

Simulation standard output — Peter Gleckler
tel: (510) 422-7631
fax: (510) 422-7675
email: gleckler@airsea.llnl.gov
or
Susan Peterson
tel: (510) 422-7682
fax: (510) 422-7675
email: susan@albedo.llnl.gov
or
Clyde Dease
tel: (510) 423-0358
fax: (510) 422-7675
email: dease@yoda.llnl.gov

Simulation history — Ken Sperber
tel: (510) 422-7720
fax: (510) 422-7675
email: sperber@space.llnl.gov

Statistical software — Ben Santer
tel: (510) 423-4249
fax: (510) 422-7675
email: bsanter@rainbow.llnl.gov

Diagnostic software — Jim Boyle
tel: (510) 422-1824
fax: (510) 422-7675
email: boyle@cobra.llnl.gov

Travel and administration — Lourdes Placeres
tel: (510) 422-7638
fax: (510) 422-7675
email: placeres1@llnl.gov
or
Anna McCravy
tel: (510) 422-8894
fax: (510) 422-7675
email: mccravy@sprite.llnl.gov